AIMS Biophysics

AIMS Biophysics, 10(3): 263–280.
DOI: 10.3934/biophy.2023018
Received: 29 June 2023
Revised: 25 August 2023
Accepted: 03 September 2023
Published: 15 September 2023

http://www.aimspress.com/journal/biophysics

Research article

Mathematical modeling for solving fractional model cancer bosom malignant growth

Shaimaa A. M. Abdelmohsen[1], D. Sh. Mohamed[2], Haifa A. Alyousef[1], M. R. Gorji[3] and Amr M. S. Mahdy[2,4,*]

[1] Department of Physics, College of Science, Princess Nourah bint Abdulrahman University, P.O. Box 84428, Riyadh 11671, Saudi Arabia
[2] Department of Mathematics, Faculty of Science, Zagazig University, Zagazig 44519, Egypt
[3] Faculty of Medicine and Health Sciences, Ghent University, Ghent 9000, Belgium
[4] Department of Mathematics, College of Science, Taif University, P.O. Box 11099, Taif 21944, Saudi Arabia

* **Correspondence:** Email: amattaya@tu.edu.sa.

Abstract: In this essay, we have presented a fractional numerical model of breast cancer stages with cardiac outcomes. Five compartments were used to build the model, each of which represented a subpopulation of breast cancer patients. Variables A, B, C, D, and E each represent a certain subpopulation. They are levels 1 and 2 (A), level 3 (B), level 4 (C), disease-free (D) and cardiotoxic (E). We have demonstrated that the fractional model has a stable solution. We also discuss how to optimally control this model and numerically simulate the control problem. Using numerical simulations, we computed the results of the dissection. The model's compartment diagram has been completed. A predictor-corrector method has been used to manage the fractional derivatives and produce numerical solutions. The Caputo sense has been used to describe fractional derivatives. The results have been illustrated through numerical simulations. Furthermore, the numerical simulations show that the cancer breast malignant growth fractional order model is easier to model than the traditional integer-order model. To compute the results, we have used mathematical programming. We have made it clear that the numerical method that was applied in this publication to solve this model was not utilized by any other author before that, nor has this method been investigated in the past. Our investigation established this approach.

Keywords: Cancer bosom malignant growth; Caputo sense; graph of a signal; optimal control;

predictor-corrector method

1. Introduction

Every woman is susceptible to breast cancer. Breast cancer is the second most lethal cancer after lung cancer, according to data from the World Health Organization (WHO) from 2004. The tumor, lymph node, metastasis (TNM) system establishes the malignancy phase [1]. The tumor size (T), the number of lymph nodes (N), and the spread (Metastasis) to other sites (M) are used by the TNM system to determine the degree of malignancy. If the cancer is identified in its early stages, the recovery from breast disease is not at all difficult. There is less chance of recovery as the stage increases. There are several different types of cancer medications, including chemotherapy, radiotherapy, hormone therapy, focused therapy and other claimed medical treatments. Cancer treatment kills cancer cells, prevents cancer cells from becoming cancer cells, or prevents cancer cells from receiving signals for cell proliferation. In this paper, we create a numerical model to analyze the effects of chemotherapy on the hearts of patients and the stages of breast cancer [2].

Models of heart failure based on the cardiotoxicity of anticancer medications are discussed in [1] and [3], dissecting cancer through mathematics: from the cell to the animal model in [4], a mathematical model analysis of breast cancer stages with heart side effects in chemotherapy patients in [5], optimal control and solution of the cellular DNA cancer model in [6], optimal control is used to study the dynamical behaviors of fractional financial awareness models in [7]. In [8], a Caputo-Fabrizio derivative is used to solve fractional glioblastoma multiforme. In [9] studies numerical, approximate solutions and optimal control of Lassa Hemorrhagic Fever in pregnant women. In [10] studies on a general formulation for numerical optimization of control problems and [11] the formulation of Euler-Lagrange equations for fractional variational problems. A formulation and numerical scheme for fractional optimal control problems are presented in [12]. In [13], fractional optimal control problems with multiple states and control variables are considered. A numerical method for solving the nonlinear equations of Emden-Fowler models is described in [14] and a numerical approach is used in optimal control [15] for a nonlinear mathematical model of the tumor under immune suppression. [16] studies optimal control for a fractional tuberculosis infection model taking diabetes and resistant strains into account and a numerical approach to fractional optimal control in the transmission dynamics of the West Nile model with state and control time delays is presented in [17]. [18] describes numerical treatments of West Nile virus transmission dynamics and optimal control. Studies on the dynamics of a fractional mathematical model of cancer tumor disease are presented in [19]. Approximate numerical methods for mathematical and physical studies for COVID-19 models are discussed in [20]. The 3-dimensional multispecies nonlinear tumor growth-I: model and numerical approach is studied in [21]. Studies [22] used symmetry approaches on a mathematical model of a brain tumor. The fractional-order susceptible-infected-susceptible (SIS) epidemic model with variable population size is described in [23]. An equation of fractional diffusion is used to simulate a cancer tumor in investigations [24]. The optimal control and spectral colocation method for solving smoking models are described in [25]. In [26], the authors present a numerical solution and dynamical behaviors for solving a fractional nonlinear rubella disease model. Dynamical behaviors of a nonlinear coronavirus (COVID-19) model with numerical studies are described in [27]. The fractional mathematical model for the concentration of tumor cells for a constant death rate has

analytical solutions in [28] research. The fractional-order mathematical model that underlies immune chemotherapeutic therapy for breast cancer was numerically investigated in studies [29] employing neural networks. A non-local tumor growth model has solutions and numerical approximations in works by [30]. The numerical solutions for a tumor cell invasion and migration model in [31] studies. Computational simulations for solving nonlinear composite oscillation fractional are described in [32]. For the chaotic-cancer-model, investigations [33] enhanced the numerical solutions. [34] studies general fractional financial models of awareness using the Caputo Fabrizio derivative. [35] studies algorithms for fractional calculus using a variety of numerical methods. [36] studies finite-time event-triggered adaptive neural control for fractional-order nonlinear systems. Event-triggered adaptive neural control of fractional-order nonlinear systems with full-state constraints is described in [37]. [38] studies adaptive asymptotic tracking of nonlinear systems with unknown virtual control coefficients using the Barrier Lyapunov function. A fractional mathematical model of the breast cancer competition model is described in [39].

We provide a brand-new fractional numerical model of the stages of bosom disease with cardiac findings that demonstrate the existence of a stable arrangement in the partial model. Additionally explored are the model's ideal control and the mathematical procedure for simulating the control problem. With the help of mathematical games, we were able to attain the investigation's results. Similar to this, when various starting conditions are applied, the mathematics have a conclusion, which is supposedly a balance point that is constantly steady without conditions.

The paper is organized as follows: A predictor-corrector approach, marking, and preliminary work have been represented in Section 2. In Section 2, we also used a signal flow diagram to illustrate the cancer model. In Section 3, we talked about the uniformly stable solution after control and the optimal control (OC) for the fractional cancer model. In Section 4, we have resolved the nonlinear fractional cancer model using a predictor-corrector approach. The cancer model has been numerically simulated in Section 5. In Section 6, conclusions have been discussed. We describe the upcoming work in Section 7.

2. Methods

2.1. Preparations and marking

The following are some essential advantages and benefits of the concept of fractional calculus that will be helpful in this paper:

Definition 2.1. In Caputo's sense, the derivative fractional (Δ^r) is [6,26,32,35]:

$$\Delta^r A(t) = \frac{1}{\Gamma(n-r)} \int_0^t (t-\eta)^{n-r-1} A^{(n)}(\eta) d\eta, \quad \text{for } n-1 < r \le n, \quad n \in \mathrm{N}. \tag{2.1}$$

Definition 2.2. [35] can be used for $r > 0$ to introduce the order derivative fractional Caputo r overall space, as Δ^r intended:

$${}^{c}\Delta_{+}^{r} A(t) = \frac{1}{\Gamma(n-r)} \int_{-\infty}^{t} (t-\eta)^{n-r-1} \Delta^n f(\eta) d\eta. \tag{2.2}$$

2.2. Predictor-corrector method algorithm

The following system of variable fractional order differential equations will be solved using the predictor-corrector method algorithm [34,35], which we shall present.

$$\begin{aligned}
&\Delta^{r_1} x(t) = A_1(x, y, z),\\
&\Delta^{r_2} y(t) = A_2(x, y, z), \qquad 0 \le t \le T.\\
&\Delta^{r_3} z(t) = A_3(x, y, z),
\end{aligned}$$

with $0 < r_j \le 1$, $(j = 1,2,3)$ and initial condition (x_0, y_0, z_0).

(1) Determine these predicted values:

$$\begin{aligned}
x_{m+1}^q &= x_0 + \sum_{j=0}^{m} \frac{\beta_{1,j,m+1}}{\Gamma\left(r_1\left(t_{m+1}\right)\right)} A_1\left(x_j, y_j, z_j\right),\\
y_{m+1}^q &= y_0 + \sum_{j=0}^{m} \frac{\beta_{2,j,m+1}}{\Gamma\left(r_2\left(t_{m+1}\right)\right)} A_2\left(x_j, y_j, z_j\right),\\
z_{m+1}^q &= z_0 + \sum_{j=0}^{m} \frac{\beta_{3,j,m+1}}{\Gamma\left(r_3\left(t_{m+1}\right)\right)} A_3\left(x_j, y_j, z_j\right),
\end{aligned}$$

where

$$\beta_{i,j,m+1} = \frac{k^{r_i}}{r_i}\left[(m-j+1)^{r_i} - (m-j)^{r_i}\right]. \quad k = \frac{T}{M}, \; T_m = mk.$$

(2) Perform the following analysis on the corrected values:

$$\begin{aligned}
x_{m+1} &= x_0 + \frac{k^{r_1}}{\Gamma\left(r_1\left(t_{m+1}\right)+2\right)} + A_1\left(x_{m+1}^q, y_{m+1}^q, z_{m+1}^q\right) + \sum_{j=0}^{m} \frac{k^{r_1}\beta_{1,j,m+1}\gamma_{1,j,m+1}}{\Gamma\left(r_1\left(t_{m+1}\right)+2\right)} A_1\left(x_j, y_j, z_j\right),\\
y_{m+1}^q &= y_0 + \frac{k^{r_2}}{\Gamma\left(r_2\left(t_{m+1}\right)+2\right)} + A_2\left(x_{m+1}^q, y_{m+1}^q, z_{m+1}^q\right) + \sum_{j=0}^{m} \frac{k^{r_1}\beta_{2,j,m+1}\gamma_{2,j,m+1}}{\Gamma\left(r_2\left(t_{m+1}\right)+2\right)} A_2\left(x_j, y_j, z_j\right), \text{ where}\\
z_{m+1}^q &= z_0 + \frac{k^{r_3}}{\Gamma\left(r_3\left(t_{m+1}\right)+2\right)} + A_3\left(x_{m+1}^q, y_{m+1}^q, z_{m+1}^q\right) + \sum_{j=0}^{m} \frac{k^{r_3}\beta_{3,j,m+1}\gamma_{3,j,m+1}}{\Gamma\left(r_3\left(t_{m+1}\right)+2\right)} A_3\left(x_j, y_j, z_j\right),
\end{aligned}$$

$$\gamma_{1,j,m+1} = \begin{cases} m^{r_i+1} - (m - r_i)(m+1)^{r_i}, & j = 0,\\ (m-j-2)^{r_i+1} + (m-j)^{r_i+1} - 2(m-j+1)^{r_i}, & 1 \le j \le m,\\ 1, & j = m+1. \end{cases}$$

See [40,41] for more information on the method.

2.3. Our proposed model

The following innovative mathematical fractional of cancer mamma stages with cardiac side effects is researched in this piece for its approximative analytical solutions at *r*. The analytical approximate solution of the fractional order cancer model is the subject of recent research [5]:

$$\begin{bmatrix}\Delta^r A\\ \Delta^r B\\ \Delta^r C\\ \Delta^r D\\ \Delta^r E\end{bmatrix}=\begin{bmatrix}\theta_1\\ \theta_2\\ \theta_3\\ 0\\ 0\end{bmatrix}+\begin{bmatrix}-(\mu_{AD}+\mu_{AB}) & 0 & 0 & 0 & 0\\ \mu_{AB} & -(\mu_{BD}+\mu_{BC}+\mu_{BC}+\gamma_2) & 0 & \mu_{BD} & 0\\ 0 & \mu_{BC} & -(\mu_{CD}+\mu_{CE}+\gamma_3) & \mu_{DC} & 0\\ \mu_{AD} & \mu_{BD} & \mu_{CD} & -(\mu_{DB}+\mu_{DC}+\mu_{DE}) & 0\\ 0 & \mu_{BE} & \mu_{CE} & \mu_{DE} & -\gamma_1\end{bmatrix}\begin{bmatrix}A\\ B\\ C\\ D\\ E\end{bmatrix}, \tag{2.3}$$

with initial conditions $A(0)=A_0, \mathrm{B}(0)=B_0, \mathrm{C}(0)=C_0, \mathrm{D}(0)=D_0$ and $E(0)=E_0$.

Five compartments representing different subpopulations of breast cancer patients were used to build the model. Variables A, B, C, D and E each represent a certain subpopulation. Patients with ductal carcinoma in situ, stages 1, 2A and 2B are represented by sub-population A. Cancer patients in stages 3A and 3B are represented by subpopulation B. Patients with stage 4 cancer make up subpopulation C. Cancer patients in subpopulation D who are free of the disease following chemotherapy are represented. Cancer cannot be observed in an environment free of sickness. Cardiotoxic cancer patients are expressed in sub-population E. In Figure 1, the sign stream diagram is displayed. A system of differential equations is used to express the rate of change for each subpopulation (1). Be aware of the set defined by $\psi=\{(A,B,C,D,E)|A>0,B>0,C>0,D>0,E>0\}$. It's important to notice that all of the parameters shown in Table 1 are taken to have positive values.

Figure 1: The signal flow diagram is a tool that may illustrate the relationships between the states of the system and give us access to graph-theoretic tools for finding novel system characteristics.

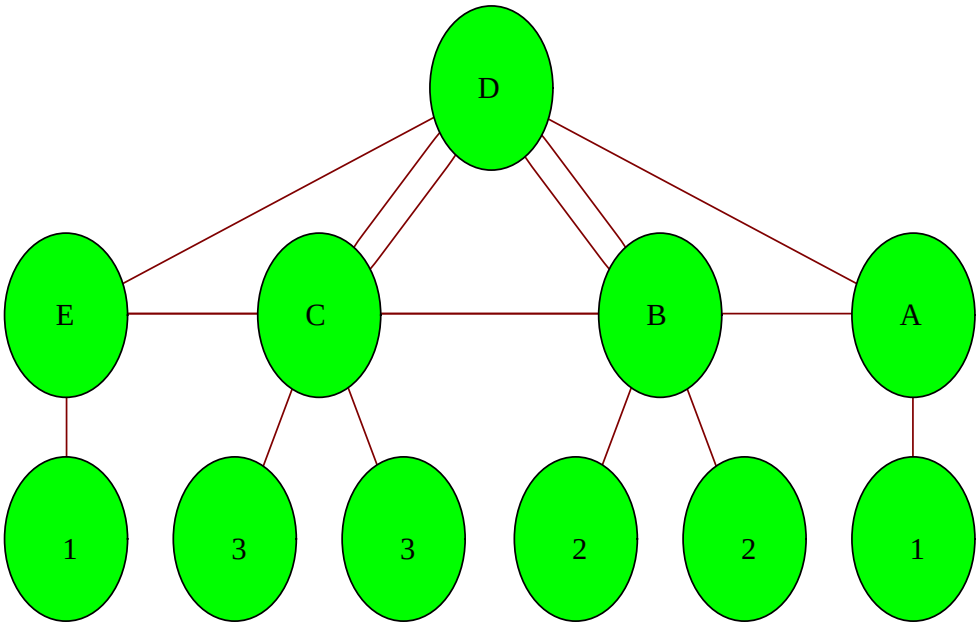

Figure 1. Graph of a signal, see [24,26,29,30].

Table 1. The physical significance and description of each parameter.

Parameter	Description
$\theta_1 = 5$	Number of patients examined to be in stages 1 and 2 of cancer
$\theta_2 = 20$	The number of patients undergoing treatment for stage 3 cancer
$\theta_3 = 11$	The number of patients examined to endure malignant growth in phase 4
$\mu_{AB} = 0.56$	Rate increased from phase 1 or 2 to stage 3 (reformist illness)
$\mu_{AD} = 0.63$	Pace of phase 1 or 2 patients who experience a total reaction
$\mu_{BD} = 0.35$	The rate at which phase 3 sick people experience a total reaction
$\mu_{BC} = 0.62$	Expanded average from phase 3 to phase 4 (reformist illness)
$\mu_{BE} = 0.3$	Pace of phase 3 malignant growth chemotherapy in sick patients who experiment with cardiotoxic treatment
$\mu_{CD} = 0.42$	Pace of Phase 4 patients undergoing total reaction
$\mu_{CE} = 0.3$	The rate of phase 4 malignant growth chemotherapy in sick patients undergoing cardiotoxic treatment
$\mu_{DB} = 0.36$	The rate of illness releases ill people who fall back to position 3
$\mu_{DC} = 0.42$	The tempo of illness releases stickers that revert to arrangement 4
$\mu_{DE} = 0.3$	Ailment release rate of sick people who experiment cardiotoxic treatment
$\gamma_1 = 0.4$	Cardiotoxic patients are dying at a faster rate
$\gamma_2 = 0.5$	Patients with stage 3 malignant growth are dying at a faster rate
$\gamma_3 = 0.8$	Patients with stage 4 malignant growth are dying at a faster rate

3. Numerical modeling

3.1. Optimal control for the fractional cancer model

This section explains the ideal control for the fractional cancer system.

$$\begin{aligned}
\Delta^r A &= \theta_1 - \mu_{AD}A - \mu_{AB}A,\\
\Delta^r B &= \theta_2 + \mu_{AB}A + \mu_{DB}D - \mu_{BD}B - \mu_{BC}B - \mu_{BE}B - \gamma_2 B,\\
\Delta^r C &= \theta_3 + \mu_{BC}B + \mu_{DC}D - \mu_{CD}C - \mu_{CE}C - \gamma_3 C,\\
\Delta^r D &= \mu_{AD}A + \mu_{BD}B + \mu_{CD}C - \mu_{DB}D - \mu_{DC}D - \mu_{DE}D,\\
\Delta^r E &= \mu_{DE}D + \mu_{CE}C + \mu_{BE}B - \gamma_1 E.
\end{aligned} \tag{3.1.1}$$

The equations (3.1.1) in R^5, generated from references [11–15,18–21,29], will be explained as follows: $\forall t \in [0, T_f] = [0,1]$, $\Omega = \left\{ (\mu_{CD}, \mu_{BE}) \in \left(L^\infty \times L^\infty \right) \middle| \, 0 \le \mu_{CD}, \mu_{BE} \le 1 \right\}$,

where T_f is time final, $\mu_{CD}(.)$ is the typical value of phase 4 patients testing a complete echo and $\mu_{BE}(.)$ is the average number of cancer patients receiving phase 3 chemotherapy who test for cardiotoxicity. $\mu_{CD}(.)$ and $\mu_{BE}(.)$ are the mechanisms for control. The standard is the space function L^∞ $\|t\|_\infty = \max_j |t_j|$.

The functional goal was described as follows:

$$J = \int_0^{T_f} \left[b_1 A + b_2 \mu_{CD}^2 + b_3 \mu_{BE}^2 \right] dt, \tag{3.1.2}$$

where b_1, b_2 and b_3 reflect the average of phase 3 cancer chemotherapy patients who experience cardiotoxicity and the measure of stage 4 patients who experiment with a full echo, respectively.

There are defined minimize functions

$$J = \int_0^{T_f} \phi \, dt, \tag{3.1.3}$$

where $\phi = \left[a_1 A(t) + a_2 \mu_{CD}^2(t) + a_3 \mu_{BE}^2(t) \right]$,

bound by the constraint

$$\Delta^r A = \varepsilon_1, \quad \Delta^r B = \varepsilon_2, \quad \Delta^r C = \varepsilon_3, \quad \Delta^r D = \varepsilon_4, \quad \Delta^r E = \varepsilon_5, \tag{3.1.4}$$

where $\varepsilon_j = \varepsilon\left(A, B, C, D, E, \mu_{CD}, \mu_{BE}, t\right), \qquad j = 1,2,3,4,5,$

met the initial cases' requirements:

$$A(0) = A_1, \quad B(0) = B_1, \quad C(0) = C_1, \; D(0) = D_1, \; E(0) = E_1. \tag{3.1.5}$$

For the objective of the fractional optimal control problem (FOCP), see [26–29]:

$$J^* = \int_0^{T_f} \left[H - \sum_{i=1}^{5} \lambda_i \varepsilon_i \right] dt. \tag{3.1.6}$$

The control equation (3.1.1) and objective Hamiltonian (3.1.6) are shown be pursuing the following goals:

$$H = \phi + \sum_{i=1}^{5} \lambda_i \varepsilon_i, \tag{3.1.7}$$

Therefore

$$\begin{aligned} H =& a_1 A + a_2 \mu_{CD}^2 + a_3 \mu_{BE}^2 + \lambda_1 \left[\theta_1 - \mu_{AD} A - \mu_{AB} A \right] \\ &+ \lambda_2 \left[\theta_2 + \mu_{AB} A + \mu_{DB} D - \mu_{BD} B - \mu_{BC} B - \mu_{BE} B - \gamma_2 B \right] \\ &+ \lambda_3 \left[\theta_3 + \mu_{BC} B + \mu_{DC} D - \mu_{CD} C - \mu_{CE} C - \gamma_3 C \right] \\ &+ \lambda_4 \left[\mu_{AD} A + \mu_{BD} B + \mu_{CD} C - \mu_{DB} D - \mu_{DC} D - \mu_{DE} D \right] \\ &+ \lambda_5 \left[\mu_{DE} D + \mu_{CE} C + \mu_{BE} B - \gamma_1 E \right]. \end{aligned} \tag{3.1.8}$$

In [26–29] describe the necessary and sufficient conditions.

$$\Delta^r \lambda_1 = \frac{\partial H}{\partial A}, \quad \Delta^r \lambda_2 = \frac{\partial H}{\partial B}, \quad \Delta^r \lambda_3 = \frac{\partial H}{\partial C}, \quad \Delta^r \lambda_4 = \frac{\partial H}{\partial D}, \quad \Delta^r \lambda_5 = \frac{\partial H}{\partial E}, \tag{3.1.9}$$

$$\frac{\partial H}{\partial u_r} = 0, \quad r = 1, \ 2 \Rightarrow \quad \frac{\partial H}{\partial u_1} = 0, \quad \frac{\partial H}{\partial u_2} = 0, \tag{3.1.10}$$

$$\Delta^r A = \frac{\partial H}{\partial \lambda_1}, \quad \Delta^r B = \frac{\partial H}{\partial \lambda_2}, \quad \Delta^r C = \frac{\partial H}{\partial \lambda_3}, \quad \Delta^r D = \frac{\partial H}{\partial \lambda_4}, \quad \Delta^r E = \frac{\partial H}{\partial \lambda_5}, \tag{3.1.11}$$

furthermore,

$$\lambda_i, (T_f) = 0, \tag{3.1.12}$$

where λ_i, $i = 1,2,3,4,5$ are the Lagrange multipliers. The following theorem completes our finding:

Theorem 1.

If μ_{CD} and μ_{BE} are optimal controls with alike states A^*, B^*, C^*, D^* and E^*, then there dwell adjoint variables $\lambda_j^*, \quad j = 1,2,3,4,5,$ which satisfy the following requirements:

(i) Equations adjoint

The five equations below can be created by combining the criteria in the text theorem with equations (3.1.9) shown ([26–29]).

$$\Delta^r \lambda_1^* = a_1 + \lambda_1^* \left[-\mu_{AD} - \mu_{AB} \right] + \lambda_2^* \left[\mu_{AB} \right] + \lambda_4^* \left[\mu_{AD} \right], \tag{3.1.13}$$

$$\Delta^r \lambda_2^* = \lambda_2^* \left[-\mu_{BD} - \mu_{BC} - \mu_{BE} - \gamma_2 \right] + \lambda_3^* \left[\mu_{BC} \right] + \lambda_4^* \left[\mu_{BD} \right] + \lambda_5^* \left[\mu_{BE} \right], \tag{3.1.14}$$

$$\Delta^r \lambda_3^* = \lambda_3^* \left[-\mu_{CD} - \mu_{CE} - \gamma_3 \right] + \lambda_4^* \left[\mu_{CD} \right] + \lambda_5^* \left[\mu_{CE} \right], \tag{3.1.15}$$

$$\Delta^r \lambda_4^* = \lambda_2^* \left[\mu_{DB} \right] + \lambda_3^* \left[\mu_{DC} \right] + \lambda_4^* \left[-\mu_{DB} - \mu_{DC} - \mu_{DE} \right] + \lambda_5^* \left[\mu_{DE} \right], \tag{3.1.16a}$$

$$\Delta^r \lambda_4^* = \lambda_5^* \left[-\gamma_1 \right]. \tag{3.1.16b}$$

(ii) Condition of transversality:

$$\lambda_j^*(T_f) = 0. \tag{3.1.17}$$

(iii) **Condition of optimality**

$$H = \min_{0 \le \mu_{CD}^*, \mu_{BE}^* \le 1} H^*. \tag{3.1.18}$$

Additionally, the functions regulate the equations in (3.1.10) by adding equations for u_1^*, u_2^* are acquired as

$$\mu_{CD} = \frac{C^* \left[\lambda_3^* - \lambda_4^* \right]}{2a_2}, \tag{3.1.19}$$

$$\mu_{BE} = \frac{B^* \left[\lambda_2^* - \lambda_5^* \right]}{2a_2}, \tag{3.1.20}$$

$$\mu_{CD}^* = \min \left\{ 1, \quad \max \left\{ 0, \frac{C^* \left[\lambda_3^* - \lambda_4^* \right]}{2a_2} \right\} \right\}, \tag{3.1.21}$$

$$\mu_{BE}^* = \min \left\{ 1, \quad \max \left\{ 0, \frac{B^* \left[\lambda_2^* - \lambda_5^* \right]}{2a_2} \right\} \right\}. \tag{3.1.22}$$

Reasoning. Eqs. (3.1.11) through (3.1.16) of the co-state system, where the Hamiltonian is found H^* is given by

$$H^* = a_1 A^* + a_2 \mu_{CD}^{*2} + a_3 \mu_{BE}^{*2} + \lambda_1^* D^q A^* + \lambda_2^* D^q B^* + \lambda_3^* D^q C^* + \lambda_4^* D^q D^* + \lambda_4^* D^q E^*. \tag{3.1.23}$$

Then, Eq. (3.1.12)'s case satisfied, and Eqs. (3.1.21)–(3.1.22)'s optimal control can be deduced from Eq (3.1.10). Starting to put $u_j^*, \ j = 1, 2$ in Eq (3.1.1), moreover

$$
\begin{aligned}
\Delta^r A^* &= \theta_1 - \mu_{AD}A^* - \mu_{AB}A^*,\\
\Delta^r B^* &= \theta_2 + \mu_{AB}A^* + \mu_{DB}D^* - \mu_{BD}B^* - \mu_{BC}B^* - \mu^*_{BE}B^* - \gamma_2 B^*,\\
\Delta^r C^* &= \theta_3 + \mu_{BC}B^* + \mu_{DC}D^* - \mu^*_{CD}C^* - \mu_{CE}C^* - \gamma_3 C^*,\\
\Delta^r D^* &= \mu_{AD}A^* + \mu_{BD}B^* + \mu^*_{CD}C^* - \mu_{DB}D^* - \mu_{DC}D^* - \mu_{DE}D^*,\\
\Delta^r E^* &= \mu_{DE}D^* + \mu_{CE}C^* + \mu^*_{BE}B^* - \gamma_1 E^*.
\end{aligned}
\tag{3.1.24}
$$

Refer to the references for more information on optimal control fractional [11–15,18–21,29].

3.2. Existence solution (after control)

This section will demonstrate the existence of the solution to the system Eqs (3.1.13)-(3.1.16), which can be found in [24,26,28,30] as follows:
Let

$$w_1 = a_1 + \lambda_1^*\left[-\mu_{AD} - \mu_{AB}\right] + \lambda_2^*\left[\mu_{AB}\right] + \lambda_4^*\left[\mu_{AD}\right],$$

$$w_2 = \lambda_2^*\left[-\mu_{BD} - \mu_{BC} - \mu_{BE} - \gamma_2\right] + \lambda_3^*\left[\mu_{BC}\right] + \lambda_4^*\left[\mu_{BD}\right] + \lambda_5^*\left[\mu_{BE}\right],$$

$$w_3 = \lambda_3^*\left[-\mu_{CD} - \mu_{CE} - \gamma_3\right] + \lambda_4^*\left[\mu_{CD}\right] + \lambda_5^*\left[\mu_{CE}\right],$$

$$w_4 = \lambda_2^*\left[\mu_{DB}\right] + \lambda_3^*\left[\mu_{DC}\right] + \lambda_4^*\left[-\mu_{DB} - \mu_{DC} - \mu_{DE}\right] + \lambda_5^*\left[\mu_{DE}\right],\ w_5 = \lambda_5^*\left[-\gamma_1\right].$$

Let $\Phi = \left\{\lambda_j^{\#} \in R : \left|\lambda_j^{\#}\right| \le c,\ j = 1,2,3,4,5,\quad t \in [0,T\right\}$.

At Φ :
$\frac{\partial w_1}{\partial \lambda_1^*} = \left[-\mu_{AD} - \mu_{AB}\right]$, $\frac{\partial w_1}{\partial \lambda_2^*} = \left[\mu_{AB}\right]$, $\frac{\partial w_1}{\partial \lambda_3^*} = 0$, $\frac{\partial w_1}{\partial \lambda_4^*} = \left[\mu_{AD}\right]$, $\frac{\partial w_1}{\partial \lambda_5^*} = 0$,

$\frac{\partial w_2}{\partial \lambda_1^*} = 0$, $\frac{\partial w_2}{\partial \lambda_2^*} = \left[-\mu_{BD} - \mu_{BC} - \mu_{BE} - \gamma_2\right]$,

$\frac{\partial w_2}{\partial \lambda_3^*} = \left[\mu_{BC}\right]$, $\frac{\partial w_2}{\partial \lambda_4^*} = \left[\mu_{BD}\right]$, $\frac{\partial w_2}{\partial \lambda_5^*} = \left[\mu_{BE}\right]$,

$\frac{\partial w_3}{\partial \lambda_1^*} = 0$, $\frac{\partial w_3}{\partial \lambda_2^*} = 0$, $\frac{\partial w_3}{\partial \lambda_3^*} = \left[-\mu_{CD} - \mu_{CE} - \gamma_3\right]$, $\frac{\partial w_3}{\partial \lambda_4^*} = \left[\mu_{CD}\right]$, $\frac{\partial w_3}{\partial \lambda_5^*} = \left[\mu_{CE}\right]$,

$\frac{\partial w_4}{\partial \lambda_1^*} = 0$, $\frac{\partial w_4}{\partial \lambda_2^*} = \left[\mu_{DB}\right]$, $\frac{\partial w_4}{\partial \lambda_3^*} = \left[\mu_{DC}\right]$, $\frac{\partial w_4}{\partial \lambda_4^*} = \left[-\mu_{DB} - \mu_{DC} - \mu_{DE}\right]$, $\frac{\partial w_4}{\partial \lambda_5^*} = \left[\mu_{DE}\right]$,

$$\left|\frac{\partial w_1}{\partial \lambda_1^*}\right| \le c_{11},\ \left|\frac{\partial w_1}{\partial \lambda_2^*}\right| \le c_{12},\ \left|\frac{\partial w_1}{\partial \lambda_3^*}\right| \le c_{13},\ \left|\frac{\partial w_1}{\partial \lambda_4^*}\right| \le c_{14},\ \left|\frac{\partial w_1}{\partial \lambda_5^*}\right| \le c_{15},$$

$$\left|\frac{\partial w_2}{\partial \lambda_1^*}\right| \le c_{21}, \quad \left|\frac{\partial w_2}{\partial \lambda_2^*}\right| \le c_{22}, \quad \left|\frac{\partial w_2}{\partial \lambda_3^*}\right| \le c_{23}, \quad \left|\frac{\partial w_2}{\partial \lambda_4^*}\right| \le c_{24}, \quad \left|\frac{\partial w_2}{\partial \lambda_5^*}\right| \le c_{25},$$

$$\left|\frac{\partial w_3}{\partial \lambda_1^*}\right| \le c_{31}, \quad \left|\frac{\partial w_3}{\partial \lambda_2^*}\right| \le c_{32}, \quad \left|\frac{\partial w_3}{\partial \lambda_3^*}\right| \le c_{33}, \quad \left|\frac{\partial w_3}{\partial \lambda_4^*}\right| \le c_{34}, \quad \left|\frac{\partial w_3}{\partial \lambda_5^*}\right| \le c_{35},$$

$$\left|\frac{\partial w_4}{\partial \lambda_1^*}\right| \le c_{41}, \quad \left|\frac{\partial w_4}{\partial \lambda_2^*}\right| \le c_{42}, \quad \left|\frac{\partial w_4}{\partial \lambda_3^*}\right| \le c_{43}, \quad \left|\frac{\partial w_4}{\partial \lambda_4^*}\right| \le c_{44}, \quad \left|\frac{\partial w_4}{\partial \lambda_5^*}\right| \le c_{45},$$

$$\left|\frac{\partial w_5}{\partial \lambda_1^*}\right| \le c_{51}, \quad \left|\frac{\partial w_5}{\partial \lambda_2^*}\right| \le c_{52}, \quad \left|\frac{\partial w_5}{\partial \lambda_3^*}\right| \le c_{53}, \quad \left|\frac{\partial w_5}{\partial \lambda_4^*}\right| \le c_{54}, \quad \left|\frac{\partial w_5}{\partial \lambda_5^*}\right| \le c_{55},$$

where: $c_{11}, c_{12}, c_{13}, c_{14}, c_{15}, c_{21}, c_{22}, c_{23}, c_{24}, c_{25}, c_{31}, c_{32}, c_{33}, c_{34}, c_{35}, c_{41}, c_{42}, c_{43}, c_{44}, c_{45},$ and $c_{51}, c_{52}, c_{53}, c_{54}, c_{55},$ have positive constants. This implies that each of the five roles f_1, f_2, f_3, f_4 and f_5 have the Lipschitz case exception. See for more information about the presence and distinction [24,26,28–30].

4. Implementation of numerical simulation

The numerical solution of the model Eq (2.3) using the GABM approach is related to this section. Following is a description of the model Eq (2.3)'s numerical methodology using GABMM:

$$A_k(t_{n+1}) = A_0 + \frac{h^q}{\Gamma(q+2)}\left[g_1\left(t_{n+1}, A_k^p, B_k^p, C_k^p, D_k^p, E_k^p\right)\right] + \sum_{r=0}^{n} b_{r,n+1} g_1\left(t_r, A_r(t_r), B_r(t_r), C_r(t_r), D_r(t_r), E_r(t_r)\right),$$

$$B_k(t_{n+1}) = B_0 + \frac{h^q}{\Gamma(q+2)}\left[g_2\left(t_{n+1}, A_k^p, B_k^p, C_k^p, D_k^p, E_k^p\right)\right] + \sum_{r=0}^{n} b_{r,n+1} g_2\left(t_r, A_r(t_r), B_r(t_r), C_r(t_r), D_r(t_r), E_r(t_r)\right),$$

$$C_k(t_{n+1}) = C_0 + \frac{h^q}{\Gamma(q+2)}\left[g_3\left(t_{n+1}, A_k^p, B_k^p, C_k^p, D_k^p, E_k^p\right)\right] + \sum_{r=0}^{n} b_{r,n+1} g_3\left(t_r, A_r(t_r), B_r(t_r), C_r(t_r), D_r(t_r), E_r(t_r)\right),$$

$$D_k(t_{n+1}) = D_0 + \frac{h^q}{\Gamma(q+2)}\left[g_4\left(t_{n+1}, A_k^p, B_k^p, C_k^p, D_k^p, E_k^p\right)\right] + \sum_{r=0}^{n} b_{r,n+1} g_4\left(t_r, A_r(t_r), B_r(t_r), C_r(t_r), D_r(t_r), E_r(t_r)\right),$$

$$E_k(t_{n+1}) = E_0 + \frac{h^q}{\Gamma(q+2)}\left[g_5\left(t_{n+1}, A_k^p, B_k^p, C_k^p, D_k^p, E_k^p\right)\right] + \sum_{r=0}^{n} b_{r,n+1} g_5\left(t_r, A_r(t_r), B_r(t_r), C_r(t_r), D_r(t_r), E_r(t_r)\right),$$

then

$$A_k^p(t_{n+1}) = A_0 + \frac{1}{\Gamma(q)}\sum_{r=0}^{n} b_{r,n+1} g_1\left(t_r, A_r(t_r), B_r(t_r), C_r(t_r), D_r(t_r), E_r(t_r)\right),$$

$$B_k^p(t_{n+1}) = B_0 + \frac{1}{\Gamma(q)}\sum_{r=0}^{n} b_{r,n+1} g_2\left(t_r, A_r(t_r), B_r(t_r), C_r(t_r), D_r(t_r), E_r(t_r)\right),$$

$$C_k^p(t_{n+1}) = C_0 + \frac{1}{\Gamma(q)}\sum_{r=0}^{n} b_{r,n+1} g_3\left(t_r, A_r(t_r), B_r(t_r), C_r(t_r), D_r(t_r), E_r(t_r)\right),$$

$$C_k^p(t_{n+1}) = D_0 + \frac{1}{\Gamma(q)}\sum_{r=0}^{n} b_{r,n+1} g_4\left(t_r, A_r(t_r), B_r(t_r), C_r(t_r), D_r(t_r), E_r(t_r)\right),$$

$$E_k^p(t_{n+1}) = E_0 + \frac{1}{\Gamma(q)}\sum_{r=0}^{n} b_{r,n+1} g_5\left(t_r, A_r(t_r), B_r(t_r), C_r(t_r), D_r(t_r), E_r(t_r)\right),$$

where

g_1, g_2, g_3, g_4, g_5 can be calculated via using the points $t_j = jk,\ j = 0,1,2,\ldots,r$

$$g_1 = \theta_1 - \mu_{AD}A - \mu_{AB}A,$$
$$g_2 = \theta_2 + \mu_{AB}A + \mu_{DB}D - \mu_{BD}B - \mu_{BC}B - \mu_{BE}B - \gamma_2 B,$$
$$g_3 = \theta_3 + \mu_{BC}B + \mu_{DC}D - \mu_{CD}C - \mu_{CE}C - \gamma_3 C,$$
$$g_4 = \mu_{AD}A + \mu_{BD}B + \mu_{CD}C - \mu_{DB}D - \mu_{DC}D - \mu_{DE}D,$$
$$g_5 = \mu_{DE}D + \mu_{CE}C + \mu_{BE}B - \gamma_1 E.$$

5. Numerical and simulation outcomes

This section uses the GABMM with values for the values and parameters that are consistent with Table 1 to provide feedback on the numerical results of the fractional-order model Eq (2.3). This approach is very effective at producing numerical FODE solutions.

Here, we've provided numerical simulations that emulate mathematical concepts utilizing the GABMM method. In Figures 2 and 3, we depict the behavior that gave rise to the models at various q.

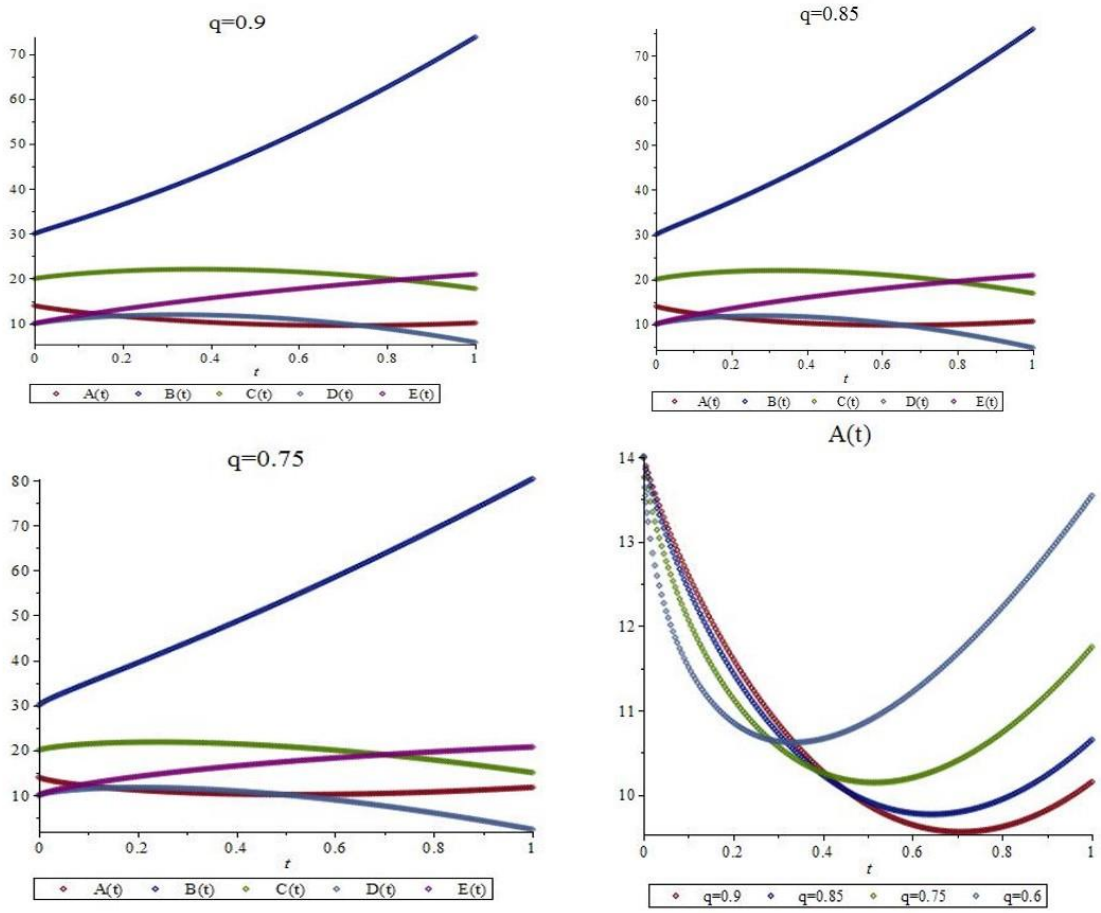

Figure 2. The connection between whole variables at q=0.9, 0.85, 0.75. The variable *A(t)* with various q.

The effectiveness of the existing method is greatly enhanced by counting more expressions of A(t), B(t), C(t), D(t), and E(t) using GABMM. Figures 2 and 3 show the various places' reactions. Figures 2 and 3 make the GABMM's accuracy more clear. The time-partial features of the several stages of bosom malignant growth are also shown by various estimates of alpha, with implications for the heart. With this foundational set of characteristics, the effect of cancer on different stages of breast cancer growth and its effects on the heart have been amply shown. These numbers reflect the heavy cancer patient's outlook if the disease is not cured. Mathematica 9.0 was used to carry out all mathematical recreations.

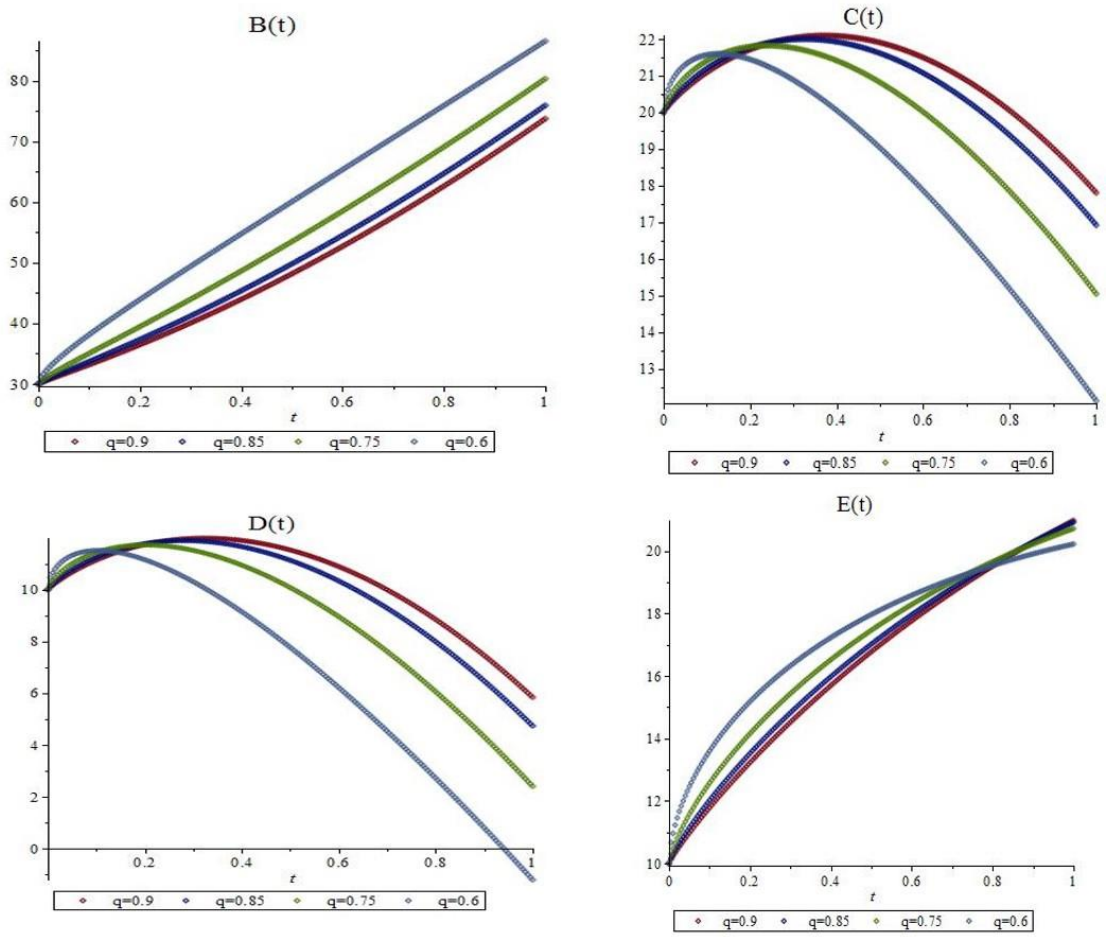

Figure 3. The variable *B(t), C(t), D(t), E(t)* with various q.

6. Conclusions

The stages of breast malignant development and their impact on the heart are examined in this research using a unique fractional numerical model. This model's ideal control is explored. The solutions that come closest to the model are obtained using the GABMM. This model's stability at its equilibrium point is investigated toward. creation of the ideal control. We introduce a numerical method for simulating the control problem. The stability analysis also discusses a numerical approach. The proposed concept can be explained using numerical simulations. The model's compartment diagrams are finished. To calculate the results, Maple 15 programming has been used.

7. Further work

In the forthcoming future work.
(a) These methods can be extended to solve other models.
(b) These methods can be extended to solve an optimal control problem for the variable-order fractional-integer mathematical model.

Use of AI tools declaration

The authors declare they have not used Artificial Intelligence (AI) tools in the creation of this article.

Data availability

In this paper, no data sets were produced or resolved in the current research data.

Acknowledgments

The authors extend their appreciation to the Deputyship for Research & Innovation, Ministry of Education in Saudi Arabia for funding this research work through the project number WE-44-0043.

Fundings

The authors extend their appreciation to the Deputyship for Research & Innovation, Ministry of Education in Saudi Arabia for funding this research work through the project number WE-44-0043.

Conflict of interest

The authors state that there are no competing interests.

Author contributions

For the lettering of this paper, all authors evenly shared, also read, and agree on the firm copy of the manuscript.

References

1. Fitzmaurice C, Dicker D, Pain A, et al. (2015) The global burden of cancer 2013. *JAMA Oncol* 1: 505–527. https://doi: 10.1001/jamaoncol.2015.0735.
2. Vasiliadis I, Kolovou G, Mikhailidis DP (2014) Cardiotoxicity and cancer therapy. *Angiology* 65: 369–371. https://doi.org/10.1177/0003319713498298
3. Mercurio V, Pirozzi F, Lazzarini E, et al. (2016) Models of heart failure based on the cardiotoxicity of anticancer drugs. *J Card Fail* 22: 449–458. https://doi.org/ 10.1016/j.cardfail.2016.04.008
4. Byrne HM (2010) Dissecting cancer through mathematics: from the cell to the animal model. *Nat Rev Cancer* 10: 221–230. https://doi.org/10.1038/nrc2808
5. Fathoni M, Gunardi G, Kusumo FA, et al. (2019) Mathematical model analysis of breast cancer stages with side effects on heart in Chemotherapy patients. *AIP Conference Proceedings* 2192: 1–9. https://doi.org/10.1063/1.5139153
6. Mohamed SM, Elagan SK, Almalki SJ, et al. (2022) Optimal control and solving of cellular DNA cancer model. *Appl Math Inform Sci* 16: 109–119. http://dx.doi.org/10.18576/amis/160111?

7. Mahdy AMS, Lotfy K, El-Bary AA (2022) Use of optimal control in studying the dynamical behaviors of fractional financial awareness models. *Soft Comput* 26: 3401–3409. https://doi.org/10.1007/s00500-022-06764-y
8. Mahdy AMS (2023) Stability existence and uniqueness for solving fractional glioblastoma multiforme using a Caputo–Fabrizio derivative. *Math Method Appl Sci* 1–18. https://doi.org/10.1002/mma.9038
9. Higazy M, El-Mesady A, et al. (2021) Numerical approximate solutions, and optimal control on the deathly Lassa Hemorrhagic fever disease in pregnant women. *J Funct Spaces* 2021: 1–15. https://doi.org/10.1155/2021/2444920
10. Mahdy AMS, Gepreel KA, Lotfy K, et al. (2023) Reduced differential transform and Sumudu transform methods for solving fractional financial models of awareness. *Appl Math J Chinese Univ* 38: 338–356. https://doi.org/10.1007/s11766-023-3713-0
11. Agrawal OP (2002) Formulation of Euler-Lagrange equations for fractional variational problems. *J Math Anal Appl* 272: 368–379. https://doi.orgS0022-247X(02)00180-4
12. Agrawal OP (2006) A formulation and numerical scheme for fractional optimal control problems. *IFAC Proc* 39: 68–72. https://doi.org/10.3182/20060719-3-PT-4902.00011
13. Agrawal OP, Defterli O, Baleanu D (2010) Fractional optimal control problems with several state and control variables. *J Vib Control* 16: 1967–1976. https://doi.org/10.1177/1077546309353361
14. Mahdy AMS (2022) A numerical method for solving the nonlinear equations of Emden-Fowler models. *J Ocean Eng Sci* In Press. https://doi.org/10.1016/j.joes.2022.04.019.
15. Sweilam NH, Al-Mekhlafi SM (2018) Optimal control for a nonlinear mathematical model of tumor under immune suppression: a numerical approach. *Optimal Control Appl Method* 39: 1581–1596. https://doi.org/10.1002/oca.2427
16. Sweilam NH, Al-Mekhlafi SM, Baleanu D (2019) Optimal control for a fractional tuberculosis infection model including the impact of diabetes and resistant strains. *J Adv Res* 17: 125–137. https://doi.org/10.1016/j.jare.2019.01.007
17. Sweilam NH, Saad OM, Mohamed DG (2019) Fractional optimal control in transmission dynamics of West Nile model with state and control time delay a numerical approach. *Adv Differ Equ* 2019: 1–25. https://doi.org/10.1186/s13662-019-2147-8
18. Sweilam NH, Saad OM, Mohamed DG (2019) Numerical treatments of the tranmission dynamics of West Nile virus and it's optimal control. *Electonic J Mat Anal Appl* 7: 9–38. https://doi.org/10.21608/ejmaa.2019.312771
19. Abaid Ur Rehman M, Ahmad J, Hassan A, et al. (2022) The dynamics of a fractional order mathematical model of cancer Ttumor disease. *Symmetry* 14: 1694. https://doi.org/10.3390/sym14081694
20. Alotaibi H, Gepreel KA, Mohamed SM, et al. (2022) An approximate numerical methods for mathematical and physical studies for covid-19 models. *Comput Syst Sci Eng* 42: 1147–1163. https://doi.org/10.32604/csse.2022.020869
21. Wise SM, Lowengrub JS, Frieboes HB, et al. (2008) Three-dimensional multispecies nonlinear tumor growth-I: model and numerical method. *J Theor Biol* 253: 524–543. https://doi.org/doi: 10.1016/j.jtbi.2008.03.027
22. Moyo S, Leach PGL (2004) Symmetry methods applied to a mathematical model of a tumour of the brain. *Proceedings of Institute of Mathematics of NAS of Ukraine* 50: 204–210.

23. El-Saka HAA (2014) The fractional order SIS epidemic model with variable population size. *J Egypt Mathematical Soc* 22: 50–54. https://doi.org/10.1016/j.joems.2013.06.006
24. Iyiola OS, Zaman FD (2014) A fractional diffusion equation model for cancer tumor. *AIP Adv* 4: 107121. https://doi.org/10.1063/1.4898331
25. Mahdy AMS, Mohamed SM, Al Amiri AY, et al. (2022) Optimal control and spectral collocation method for solving smoking models. *Intell Autom Soft Comput* 31: 899–915. https://doi.org/10.32604/iasc.2022.017801
26. Mahdy AMS, Mohamed MS, Lotfy K, et al. (2021) Numerical solution and dynamical behaviors for solving fractional nonlinear rubella ailment disease model. *Results Phys* 24: 1–10. https://doi.org/10.1016/j.rinp.2021.104091
27. Gepreel KA, Mohamed MS, Alotaibi H, et al. (2021) Dynamical behaviors of nonlinear Coronavirus (COVID-19) model with numerical studies. *Comput Mater Continua* 67: 675–686. https://doi.org/10.32604/cmc.2021.012200
28. Ahmed N, Shah NA, Ali F, et al. (2021) Analytical solutions of the fractional mathematical model for the concentration of tumor cells for constant killing rate. *Mathematics* 9: 1156. https://doi.org/10.3390/math9101156
29. Sabir Z, Munawar M, Abdelkawy MA, et al. (2022) Numerical investigations of the fractional-order mathematical model underlying immune chemotherapeutic treatment for breast cancer using the neural networks. *Fractal Fract* 6: 184. https://doi.org/10.3390/fractalfract6040184
30. Maddalena L, Ragni S (2020) Existence of solutions and numerical approximation of a non-local tumor growth model. *Math Med Biol A J IMA* 37: 58–82. https://doi.10.1093/imammb/dqz005.
31. Kolev M, Zubik KB (2011) Numerical solutions for a model of tissue invasion and migration of tumour cells. *Comput Math Methods Med* 2011: 452320. https://doi.org/10.1155/2011/452320
32. Ismail GM, Mahdy AMS, Amer YA, et al. (2022) Computational simulations for solving nonlinear composite oscillation fractional. *J Ocean Eng Sci* 1–10. https://doi.org/10.1016/j.joes.2022.06.029.
33. Yasir M, Ahmad S, Ahmed F, et al. (2017) Improved numerical solutions for chaotic-cancer-model. *AIP Adv* 7: 015110. https://doi.org/10.1063/1.4974881
34. Mahdy AMS, Amer YA, Mohamed MS, et al. (2020) General fractional financial models of awareness with Caputo Fabrizio derivative. *Adv Mechan Eng* 12: 1–9. https://doi.org/10.1177/1687814020975525
35. Diethelm K, Ford NJ, Freed AD, et al. (2005) Algorithms for the fractional calculus: a selection of numerical methods. *Comput Meth Appl Mech Eng* 194: 743–773. https://doi.org/10.1016/j.cma.2004.06.006
36. Li YX, Wei M, Tong S (2022) Event triggered adaptive neural control for fractional order nonlinear systems based on finitetime scheme. *IEEE T Cybernetics* 52: 9481–9489. https://doi.org/10.1109/TCYB.2021.3056990
37. Wei M, Li YX, Tong S (2020) Event-triggered adaptive neural control of fractional-order nonlinear systems with full-state constraints. *Neurocomputing* 412: 320–326. https://doi.org/10.1016/j.neucom.2020.06.082
38. Li YX (2020) Barrier Lyapunov function-based adaptive asymptotic tracking of nonlinear systems with unknown virtual control coefficients. *Automatica* 121: 109181. https://doi.org/10.1016/j.automatica.2020.109181

39. Solís-Pérez JE, Gómez-Aguilar JF, Atangana A (2019) A fractional mathematical model of breast cancer competition model. *Chaos, Soliton Fract* 127: 38–54. https://doi.org/10.1016/j.chaos.2019.06.027
40. Diethelm K, Ford NJ, Freed AD (2002) A predictor-corrector approach for the numerical solution of fractional differential equations. *Nonlinear Dyamics* 29: 3–22. https://doi.org/10.1023/A:1016592219341
41. Diethelm K, Ford NJ, Freed AD (2004) Detailed error analysis for a fractional adams method. *Numer Algorithms* 36: 31–52. https://doi.org/10.1023/B:NUMA.0000027736.85078.be

AIMS Press